Published in final edited form as:
Plant J. 2012 December ; 72(6): 1000–1014. doi:10.1111/tpj.12009.

Mutations in two non-canonical *Arabidopsis* SWI2/SNF2 chromatin remodeling ATPases cause embryogenesis and stem cell maintenance defects

Yi Sang[1], **Claudia O. Silva-Ortega**[2], **Shuang Wu**[1], **Nobutoshi Yamaguchi**[1], **Miin-Feng Wu**[1], **Jennifer Pfluger**[1], **C. Stewart Gillmor**[2], **Kimberly L. Gallagher**[1,*], and **Doris Wagner**[1,*]

Yi Sang: yisang@sas.upenn.edu; Claudia O. Silva-Ortega: osilva@langebio.cinvestav.mx; Shuang Wu: shuangwu@sas.upenn.edu; Nobutoshi Yamaguchi: nobuy@sas.upenn.edu; Miin-Feng Wu: miin@sas.upenn.edu; Jennifer Pfluger: jennifer@pfluger.org; C. Stewart Gillmor: sgillmor@langebio.cinvestav.mx

[1]Department of Biology, University of Pennsylvania, 415 S. University Ave, Philadelphia, PA, 19104

[2]Laboratorio Nacional de Genómica para la Biodiversidad (Langebio), CINVESTAV-IPN, Irapuato, Guanajuato, C.P 36821, MEXICO

Summary

SWI2/SNF2 chromatin remodeling ATPases play important roles in plant and metazoan development. While metazoans generally encode one or two SWI2/SNF2 ATPase genes, *Arabidopsis* encodes four such chromatin regulators: the well-studied BRAHMA and SPLAYED ATPases as well as two closely related non-canonical SWI2/SNF2 ATPases, CHR12 and CHR23. No developmental role has as yet been described for CHR12 and CHR23. Here we show that while strong single *chr12* or *chr23* mutants are morphologically indistinguishable from the wild type, *chr12 chr23* double mutants cause embryonic lethality. The double mutant embryos fail to initiate root and shoot meristems and display few and aberrant cell division. Weak double mutant embryos give rise to viable seedlings with dramatic defects in the maintenance of both the shoot and the root stem cell populations. Paradoxically, the stem cell defects are correlated with increased expression of the stem cell markers *WUSCHEL* and *WOX5*. During subsequent development, the meristem defects are partially overcome to allow for the formation of very small, bushy adult plants. Based on the observed morphological defects we named the two chromatin remodelers MINUSCULE 1 and 2. Possible links between *minu1 minu2* defects and defects in hormone signaling and replication-coupled chromatin assembly are discussed.

Keywords

stem cell maintenance; root meristem; shoot meristem; embryogenesis; chromatin remodeling; SWI2/SNF2 subgroup ATPases

[*]authors for correspondence: Doris Wagner, tel: 215-898-0483, fax: 215 898-8780, wagnerdo@sas.upenn.edu; Kimberly L. Gallagher, tel: 215 746-3605, fax: 215 898-8780, gallagkl@sas.upenn.edu.

The authors declare no conflict of interest.

Introduction

The indeterminate growth of plants requires the activities of stem cell populations located at the tips of shoots and roots. These stem cells are first initiated early in embryo development. Stem cells in the root apical meristem (RAM) are derived from the hypophyseal cell, which correlates with an auxin maximum at the base of the proembryo (Friml *et al.* 2003, Hardtke and Berleth 1998, Weijers *et al.* 2006). Following recruitment, the hypophysis divides and partitions auxin and cytokinin signals. Auxin predominates in the basal daughter cell, which will give rise to the columella initials (distal stem cells) (Muller and Sheen 2008, Weijers, *et al.* 2006). High levels of cytokinin are found in the upper daughter cell, which will become the quiescent center (QC) (Friml, *et al.* 2003, Hardtke and Berleth 1998, Muller and Sheen 2008, Weijers, *et al.* 2006). The QC is an organizing center of the RAM that is maintained by the expression of the GRAS family transcription factors, *SCARECROW* (SCR) and *SHORT-ROOT* (*SHR*), members of the PLETHORA/AINTEGUMENTA-LIKE family of transcription factors, and the homeodomain transcription factor, *WOX5* (Sarkar *et al.* 2007). Expression of *WOX5* in the QC is required to maintain columella stem cell identity (Sarkar, *et al.* 2007). In contrast, maintenance of all other stem cells in the RAM requires expression of the PLETHORA and GRAS family transcription factors (Aida *et al.* 2004, Blilou *et al.* 2005, Galinha *et al.* 2007, Helariutta *et al.* 2000, Nakajima *et al.* 2001, Sabatini *et al.* 2003). These two transcription factor families act in largely parallel pathways to direct RAM maintenance.

Establishment of the shoot apical meristem (SAM) in embryos occurs with upregulation of the expression of the homeodomain transcription factor, *WUSCHEL* (*WUS*) in response to the accumulation of auxin in the proembryo (Laux *et al.* 1996, Mayer *et al.* 1998). Next, the KNOX homeodomain transcription factor *SHOOT MERISTEMLESS* (*STM*) is upregulated, followed by induction of the *CLAVATA* genes at the heart stage of embryo development (Barton and Poethig 1993, Clark *et al.* 1996, Fletcher *et al.* 1999, Long *et al.* 1996). *CLAVATA1* (*CLV1*) and *CLAVATA3* (*CLV3*) encode for signaling pathway components. *WUS* is expressed in the SAM organizing center, just below the *CLV3* expressing population of stem cells. WUS is a positive regulator of *CLV3*, whereas CLV3 is a negative regulator of *WUS* accumulation (Brand *et al.* 2000, Fletcher, *et al.* 1999, Schoof *et al.* 2000). This negative feedback loop is thought to regulate SAM size and maintenance.

Post embryonically, both the STM and the WUS pathways maintain the SAM (Lenhard *et al.* 2002, Long, *et al.* 1996). While STM and WUS function largely in parallel, both pathways are linked to the phyotohormone cytokinin. STM promotes cytokinin biosynthesis and mutations in cytokinin receptors enhance weak *stm* mutants (Jasinski *et al.* 2005, Yanai *et al.* 2005). In addition, cytokinin is a positive regulator of *WUS* and *CLV3* expression and interacts with WUS in positive feedback loops (Buechel *et al.* 2010, Gordon *et al.* 2009, Leibfried *et al.* 2005).

The establishment and maintenance of the stem cell population is also controlled at the level of chromatin. Defects in chromatin assembly, histone acetylation and polycomb repression all cause improper SAM or RAM development (Barrero *et al.* 2007, Kaya *et al.* 2001, Kornet and Scheres 2009, Phelps-Durr *et al.* 2005, Schubert *et al.* 2006, Takeda *et al.* 2004,

Xu and Shen 2008). For example, mutations in the replication coupled chromatin assembly factor FAS1 lead to disorganized root and shoot meristems (Kaya, *et al.* 2001). In addition, stem cell identity and homeostasis in mammals and plants is linked to the activity of chromatin remodeling ATPases, including those of the SWI2/SNF subfamily (Aichinger *et al.* 2011, Ho *et al.* 2009, Kwon *et al.* 2005, Ori *et al.* 2000). SWI2/SNF2 ATPases use the energy derived from ATP hydrolysis to alter the interaction of the genomic DNA with the histone octamer, which impacts accessibility of the DNA to other proteins (Clapier and Cairns 2009).

Four SWI2/SNF2 subgroup ATPases are present in *Arabidopsis*: BRAHMA (BRM), SPLAYED (SYD), CHR12 and CHR23 (Flaus *et al.* 2006). BRM and SYD play widespread roles in *Arabidopsis* development (Bezhani *et al.* 2007, Farrona *et al.* 2004, Farrona *et al.* 2011, Hurtado *et al.* 2006, Kwon, *et al.* 2005, Kwon *et al.* 2006, Tang *et al.* 2008, Wu *et al.* 2012). Thus far, no developmental roles have been ascribed to CHR12 or CHR23. We show here that CHR12 and CHR23 belong to a single clade of non-canonical SWI2/SNF2 ATPases present in all land plants and that CHR12 and CHR23 have redundant roles in development. Strong double mutants fail to initiate both root and shoot stem cell populations, are embryonic lethal and have endosperm defects. Weak *chr12 chr23* double mutants form small, viable plants that have striking defects in SAM and RAM maintenance. Because of the observed mutant phenotypes we renamed CHR12 and CHR23 as MINUSCULE1 (MINU1) and MINU2, respectively.

Results

MINU1 and MINU2 are members of a single clade of non-canonical SWI2/SNF2 ATPases present in all tracheophytes

Using the Plaza comparative genomic tool (http://bioinformatics.psb.ugent.be/plaza/) (Proost *et al.* 2009), we identified the SWI2/SNF2 subgroup chromatin remodeling ATPases from 21 plant species. This revealed 29 homologs for the MINUSCULE (MINU) family, which includes *Arabidopsis* MINU1 (CHR12; At3g06010) and MINU2 (CHR23; At5g19310). An average number of 1.3 *MINU* genes were present per plant species. A similar low level of gene duplication was observed for the other two SWI2/SNF2 ATPases (Figure S1). Phylogenetic analyses confirmed that the plant SWI2/SNF2 subgroup ATPases (Flaus, *et al.* 2006) fall into three separate clades (Figure 1a, Figure S1): SYD, BRM and MINU.

The MINU1 and MINU2 *Arabidopsis* SWI2/SNF2 ATPases show 81.7% amino acid similarity. MINU1 and MINU2 contain a well-conserved ATPase domain (DEXDc and HELICc, Figure 1b, Figure S2)(Farrona, *et al.* 2004, Flaus and Owen-Hughes 2011, Jerzmanowski 2007), hence they likely encode functional ATPases. In their N-terminus, SWI2/SNF2 subgroup ATPases contain several conserved protein interaction domains, the QLQ domain, the helicase/SANT-associated (HSA) domain and the HSA-adjacent domain (Farrona, *et al.* 2004, Jerzmanowski 2007, Tamkun *et al.* 1992, Wu, *et al.* 2012). While MINU1 and MINU2 contain a well-conserved HSA and HSA-adjacent domain, the QLQ domain is less well conserved (Figure 1b and Figure S2)(Farrona, *et al.* 2004, Jerzmanowski 2007, Wu, *et al.* 2012). MINU1 and MINU2 also lack the C-terminal AT-hook, which has

nonspecific DNA binding activity and stabilizes the chromatin interaction of SWI2/SNF2 ATPases (Figure S2) (Farrona *et al.* 2007).

Identification of *minu1* and *minu2* loss-of-function alleles

A previous study reported a role for MINU1 in stress-induced growth arrest, but neither a T-DNA insertion line (SALK_105458, designated as *minu1-1* hereafter) nor plants over-expressing genomic *MINU1* showed visible phenotypes under normal growth conditions (Mlynarova *et al.* 2007). In order to elucidate the roles of MINU1 and MINU2 in development, we obtained several T-DNA insertion lines for both genes. Only lines, in which an insertion disrupted the corresponding mRNA, were used in this study (Figure 1b, c); these included *minu1-2* (CS413977), *minu1-3* (SALK_015562), *minu2-1* (SALK_057856) and *minu2-2* (CS904444) (Figure 1b, c). The insertion in *minu1-2* disrupts the well-conserved catalytic ATPase domain (DEXDc subdomain, Figure 1b) in the 8th exon, while the *minu1-3* insertion is present in the 3rd intron (Figure 1b). The insertions in *minu2-1* and *minu2-2* are in the 1st and 4th exons of *MINU2*, respectively (Figure 1b). Semi-quantitative RT-PCR revealed that none of the insertion alleles are RNA nulls (Figure 1c). In addition, disruption of *MINU1* did not significantly affect the expression level of *MINU2* and vice versa (Figure 1c).

MINU1 and MINU2 have redundant roles in plant development

None of the *minu1* or *minu2* homozygous mutants displayed morphological defects under normal growth conditions, suggesting that MINU1 and MINU2 likely have redundant roles in plant development. To test this idea, we crossed the *minu1* and *minu2* homozygotes to each other to yield all four possible double mutant combinations. Plants homozygous for mutations in one gene and heterozygous for mutations in the other were morphologically indistinguishable from wild type. Analysis of the progenies of these plants revealed that all combinations of double mutants exhibited embryonic defects to varying degrees (Table S1 and see below for further details). Some of the *minu1-2 minu2-1* and *minu1-3 minu2-1* embryos, but none of the *minu1-2 minu2-2* and *minu1-3 minu2-2* embryos, developed into viable adults (Table S1). The data suggest that *minu2-1* is a weaker allele than *minu2-2*. The frequency of double mutant recovery was much lower for *minu1-2 minu2-1* than for *minu1-3 minu2-1*, indicating that *minu1-2* is the stronger allele. The combined data suggest that all alleles are recessive and that MINU1 and MINU2 have redundant roles in development.

Since the recovered *minu1-2 minu2-1* and *minu1-3 minu2-1* double mutants showed similar post-embryonic phenotypes (see Figure 3 below), we used *minu1-3 minu2-1* for further analysis unless otherwise indicated. We will refer to this double mutant henceforth as *minu1 minu2* and to its wild-type-looking siblings (*minu1 minu2*/+ or *minu1* alone) as wild type.

Expression pattern of *MINU2*

Like most characterized plant chromatin regulators (see (Farrona, *et al.* 2004, Wagner and Meyerowitz 2002) for example), *MINU1* and *MINU2* were expressed in all rapidly dividing cells, including those in the embryo, and in the RAM and SAM (Figure 2a). We confirmed these data by generating *minu1-2 minu2-1* plants expressing GFP-tagged MINU2 from a genomic construct containing the native promoter that fully rescued the *minu1-2 minu 2-1*

mutants (see Figure 3b). Consistent with the public RNA expression data, GFP-tagged MINU2 protein was expressed in embryos, in the RAM and in the SAM (Figure 2b–d). Moreover, GFP-MINU2 was nuclear localized, as expected based on its predicted role as a chromatin remodeler (Figure 2b–d). GFP-MINU2 expression was much reduced in differentiated cells such as the columella (Figure 2c). Expression of GFP-MINU2 was slightly less in the QC than in the surrounding stem cells. A similar overall expression pattern was observed in reporter studies with the *MINU1* promoter (Mlynarova, *et al.* 2007).

Post-embryonic defects of *minu1 minu2* in aerial tissues

We examined morphological differences between soil-grown wild-type and *minu1 minu2* plants at 6, 10 and 16 days after planting (Figure 3a). 16% of the six-day-old *minu1 minu2* double mutants formed 3 cotyledons (Table S1 and Figure S3). On day 6 or 7, the first true leaves of wild-type plants were visible. By contrast, no true leaves were visible in *minu1 minu2* plants until they were at least 14 days old (Figure 3a and Figure S3, Figure S4). Adult soil-grown *minu1 minu2* plants showed extremely delayed development and small stature (compare Figure 3b, d). The life cycle of *minu1 minu2* was more than 3 months, while that of wild type was around 2 months (compare Figure 3b, e). When *minu1 minu2* plants bolted, they frequently formed multiple inflorescences (2.6±0.1 inflorescences per plant at ~5 cm inflorescence height, n=52), resulting in a bushy appearance (Figure 3d, e). Wild-type plants formed only one inflorescence at the same stage (~5 cm bolt). Each of these inflorescences appeared more compact than wild-type inflorescences (Figure 3c). Overall plant height was much reduced in *minu1 minu2* plants relative the wild type (compare Figure 3b, d and e). Floral development was also affected by mutations in *MINU1* and *MINU2* (Figure 3f and Table S2). The flowers that formed in *minu1 minu2* plants shortly after bolting had aborted inner organs (Figure 3f, middle panel), and did not open. Later arising *minu1 minu2* flowers had fewer stamens than wild-type flowers (3.1±0.3 compared to 5.9±0.1 in the wild type, Table S2), but no change in the number of other floral organs (Figure 3f, right panel and Table S2). In addition, the homozygous *minu1 minu2* hypomorphs had severely reduced fertility. Finally, we noted defects in phyllotaxis in *minu1 minu2* inflorescences, with more than one inflorescence initiating per node (Figure 3g).

Morphological and molecular defects of *minu1 minu2* SAMs

We decided to focus first on the delay in primary leaf initiation, which may attributable to a defect in SAM function. The SAM of six-day-old *minu1 minu2* seedlings was flat and disorganized relative to that of the wild type (Figure 4a), and consisted of large, irregularly shaped cells (Figure 4a). Periclinal divisions were frequently observed in the L2 layer (Figure 4a) of *minu1 minu2* SAMs. Ten days later, twin SAMs had formed in *minu1 minu2* plants (Figure 4b). This finding is consistent with the bushy appearance (Figure 3d, e), and the mean number of 2.6 inflorescences per *minu1 minu2* plant at bolting. The cellular organization in these later arising SAMs was more similar to that of the wild type (Figure 4b). While the twin *minu1 minu2* meristems were vegetative at day 16 (Figure 4b), the wild-type SAM had as expected already converted to an inflorescence meristem giving rise to flower primordia by this time (Yamaguchi *et al.* 2009).

To explore the molecular basis for the defects observed in *minu1 minu2*, we conducted quantitative RT-PCR (qRT-PCR) using RNA extracted from dissected shoot apices of six-day-old wild-type and *minu1 minu2* seedlings (Figure 4c). *WUS* expression was greatly elevated (~8 fold higher than wild-type levels) while *STM* mRNA expression was increased to ~2 fold of wild type. In contrast, *CLV3* and *CLV1* transcript levels were reduced to one-third and half of wild-type levels, respectively. Notably, expression of a marker of organ initiation, *AINTEGUMENTA* (*ANT)* (Long and Barton 2000), was much reduced in *minu1 minu2* (one-fifth of wild-type levels), consistent with the strong delay in initiation of the first true leaves in the double mutant (Figure 3a and 4a).

To confirm this observation and to test whether the changes we observed reflect changes in the size of the expression domain or in the level of expression per cell, we monitored expression of *WUS* and *CLV3* using well-characterized β-glucuronidase (GUS) reporter lines (Baurle and Laux 2005, Brand *et al.* 2002). In six-day-old *minu1 minu2* SAMs, *pWUS:GUS* was expressed in an expanded domain compared to the wild type (Figure 4d). The extent of the ectopic *WUS* expression varied between individual *minu1 minu2* plants (Figure S5). Expression of *pCLV3:GUS*, by contrast, was barely detectable in six-day-old *minu1 minu2* SAMs (Figure 4e). In agreement with the *pWUS:GUS* reporter expression, *in situ* RNA hybridization using a *WUS* probe showed multiple ectopic foci of *WUS* expression on independent sections of a single ten-day-old *minu1 minu2* meristem, including one in the axil of the cotyledon (Figure 4f). *WUS* expression was generally absent from its normal domain of expression. We propose that the individual foci observed by in situ hybridization together form the broad domain of expression observed by whole mount analysis with *pWUS:GUS* (Figure 4d, Figure S5).

To test if the increased *WUS* accumulation in six-day-old seedlings was responsible for the morphological defect of *minu1 minu2* SAMs, we constructed *wus minu1 minu2* triple mutants. The SAMs of the triple mutants were similarly disorganized as those of *minu1 minu2* double mutants (Figure 4a, g). Removing a negative regulator of *WUS* accumulation, CLV3, also did not rescue the *minu1 minu2* SAM defects (Figure 4a, g). Visual inspection of single, double, and triple mutant plants at day 8 and day14 of development, did not reveal any rescue of the *minu1 minu2* leaf initiation defect upon removal of *CLV3* or *WUS* activity (Figure S4). The combined data suggest that the *WUS* misexpression is likely not the cause of the reduced SAM activity in *minu1 minu2* seedlings. To test this hypothesis further, we examined *pWUS:GUS* and *pCLV3:GUS* accumulation in four- and five-day-old *minu1 minu2* shoot apices. We found no detectable *pWUS:GUS* or *pCLV3:GUS* signal at day four, with weak *pWUS:GUS*, but not *pCLV3:GUS* expression visible at day five (Figure S5).

Post-embryonic defects in below ground tissues of *minu1 minu2*

The roots of *minu1 minu2* were much shorter than those of wild-type plants (Figure 5a, b), the RAM had far fewer cells than wildtype (19.7±3.8 cells in each cortical cell file versus 26.7±3.8 cells) (Figure 5c). To determine whether the short root phenotype of *minu1 minu2* was caused by reduced cell expansion or defective cell division or both, we conducted cell flux analysis (Beemster and Baskin 1998). During the sixth day after stratification, wild-type roots grew 8.6±0.2 mm, while *minu1 minu2* roots grew 1.3±0.5 mm (Table S3). The length

of the mature cortical cells in the *minu1 minu2* mutant was only about one-half of wildtype (87.8±4.0 μm versus 159.1±10.4 μm) (Table S3). From these data, we conclude that 54.2 cells were produced during day six in the cortical cell files of wild-type roots, but only 14.6 cells in *minu1 minu2*. Hence loss of both *MINU1* and *MINU2* gene function substantially impairs the cell division rate in the root meristem, with a moderate effect on cell expansion.

Examination of the cellular patterning in five-day-old wild-type and *minu1 minu2* roots revealed a disorganized RAM in the double mutant (Figure 5d), with the QC difficult to identify. In addition, aberrantly oriented divisions were observed in the *minu1 minu2* columella that lead to a disruption of the regular columella cell layers (Figure 5d). Sporadic defects in the orientation of cell division planes were also observed in the ground tissue of *minu1 minu2* roots (Figure 5d; Figure S6).

Molecular defects in the *minu1 minu2* RAM

To examine the molecular basis for the defects in *minu1 minu2* double mutant, we extracted RNA from dissected six-day-old root tips for qRT-PCR. *minu1 minu2* accumulated *WOX5* transcript to 15 times the level of the wild type, while expression of *SHR* and *SCR* was slightly reduced (~75% of wild type) (Figure 6a). We validated these findings using well-characterized reporter lines (Blilou, *et al.* 2005, Friml, *et al.* 2003, Gallagher *et al.* 2004, Nakajima, *et al.* 2001). The *pWOX5:GFP* expression domain was expanded proximally in *minu1 minu2*, roots with low expression in the presumptive QC (Figure 6b). Overall *pSHR:SHR-GFP* and *pSCR:SCR-GFP* showed slightly reduced expression levels (Figure 6c, d) and were often absent from the presumptive QC cells. Since auxin levels are of critical importance for RAM stem cell initiation and maintenance, we also monitored the expression of the auxin response reporter *DR5rev:GFP* (Friml, *et al.* 2003). We observed reduced *DR5rev:GFP* expression in QC cells of *minu1 minu2* roots compared to wild type (Figure 6e). *DR5rev:GFP* was still expressed in the columella cells of *minu1 minu2* roots, albeit at lower levels than in the wild type.

These data suggested that QC identity is not properly maintained in the double mutant. To further probe this hypothesis, we crossed two additional QC marker lines, *QC184* and *QC25* (Sarkar, *et al.* 2007) into *minu1 minu2*/+ plants. *QC184* expression in *minu1 minu2* roots was diffuse and ectopic (Figure 6f). In contrast, *QC25* was not expressed in *minu1 minu2* roots (Figure 6g). The observed QC marker expression defects were similar to those described for *scr* mutants, which display loss of *QC25* but retain *QC184* expression (Sabatini, *et al.* 2003). The combined data validate our hypothesis that QC identity is not properly maintained in *minu1 minu2* double mutants. In addition, we note that the distal stem cells, the columella initials and occasionally even the presumptive QC region cells showed starch accumulation, which normally occurs only in differentiated columella cells (Figure 6f, g). Since WOX5 prevents differentiation of the distal stem cells (Sarkar, *et al.* 2007), these data point to a defect in WOX5 activity.

Defects in cell proliferation in *minu1 minu2* root and shoot apices

To monitor the number of dividing cells in the *minu1 minu2* RAM, we used the cell G2-M phase cycle marker *pCYCB1;1:CYCB1;1-GUS* (Colon-Carmona *et al.* 1999). This revealed

fewer actively dividing cells in *minu1 minu2* double mutant than in wild-type roots (Figure 7a). In addition, the zone of active cell division was shifted apically towards the QC in *minu1 minu2* plants (inset Figure 5a). To probe more generally for a defect in cell proliferation, we examined expression of genes linked to cell cycle progression in root and shoot apices of *minu1 minu2* seedlings relative to the wild type by qRT-PCR. We found a reduction in the expression of genes regulating all phases of the cell cycle in *minu1 minu2* apices (Figure 7b). The combined data suggest that *minu1 minu2* plants have defects in cell proliferation.

Many aspects of the *minu1 minu2* phenotype are reminiscent of mutants in cytokinin signaling (Skylar *et al.* 2010). For example, the morphological defects of *minu1 minu2* seedlings grown on agar plates in the absence of sucrose or on soil were much more severe than those in plants grown on agar plates containing sucrose (Figure S7, Figure S3 and Figure 3a). We therefore crossed two reporters whose expression is strongly cytokinin-dependent (*pARR5:GUS* and *pARR7:GUS*) (Brenner *et al.* 2012, D'Agostino *et al.* 2000, Jeon *et al.* 2010) to *minu1 minu 2* plants. We observed reduced expression for *pARR5:GUS* and *pARR7:GUS* in the SAM and in the RAM of *minu1 minu2*, relative to wild type at day six (Figure 7c, d). Taken together with the reduced *DR5rev:GFP* expression (Figure 6e), the data suggest that loss of MINU activity may cause defects in hormone signaling and homeostasis in meristems.

MINU2 can associate with chromatin

Given the noncanonical nature of MINU1 and MINU2 SWI2/SNF2 ATPases, we wished to determine whether these factors, like BRM and SYD (Kwon, *et al.* 2005, Tang, *et al.* 2008, Wu, *et al.* 2012), can be recruited to chromatin. We used six-day-old wild-type (not carrying a transgene) and *minu1 minu2* seedlings rescued by the *pMINU2:GFP-MINU2* transgene for chromatin immunoprecipitation to assess MINU2 binding to the *WUS* and the *WOX5* regulatory regions. We were unable to see MINU2 association with any of the *WUS* regulatory regions tested, but did see MINU2 association with the *WOX5* promoter region (Figure S8), suggesting that MINU2 can indeed associate with chromatin.

Embryogenesis requires presence of one functional MINU SWI2/SNF2 ATPase

Compared to the wild type, all single *minu* mutants displayed essentially normal embryo development (Table 1). By contrast, embryos produced by plants homozygous mutant for one gene and heterozygous for the other displayed severe defects in embryo development; the severity of the embryo defect was correlated with the mutant allele strength (*minu1-2 minu2-2 > minu1-3 minu2-2 > minu 1-2 minu2-1 >minu1-3 minu2-1;* Table 1)

We performed a detailed morphological analysis of embryo development at four developmental stages (the mid globular stage, mid heart stage, late torpedo stage, and late bent cotyledon stage) in both the weakest (*minu1-3 minu2-1*) and the strongest (*minu1-2 minu2-2*) double mutant combinations relative to the wild type (Figure 8a–d).

At the equivalent stages (Figure 8e–h), hypomorphic *minu1-3 minu2-1* embryos were retarded in their development. In all cases, endosperm nuclei were enlarged, irregularly

spaced and there was little evidence of endosperm cellularization (compare wild-type nuclei and cell walls in Fig. 8b with *minu1-3 minu2-1* enlarged nuclei and lack of cell walls in Fig. 8f). Ovules containing mutant embryos were smaller throughout development. At the mid globular stage, *minu1-3 minu2-1* resembled a late dermatogen stage wild-type embryo: the hypophyseal cell had not yet divided and there were no divisions in the upper tier cells that will form the SAM. At the wild type mid heart stage, *minu1-3 minu 2-1* embryos contained enlarged cells (Figure 8f), and were approximately at the early globular stage of development. At the wild-type late torpedo stage, two classes of embryos were observed in *minu1-3 minu2-1/+* siliques: 17% of the embryos had an early torpedo morphology, while 10% had a enlarged heart stage morphology (Figure 8g). Organized SAMs and RAMs had formed in both classes of mutants, albeit with fewer cells than in their wild-type counterparts. At the bent cotyledon stage, *minu1-3 minu2-1* embryos were still smaller than wild-type embryos, but morphologically normal (Figure 8h). The RAM and SAM of *minu1-3 minu2-1* embryos looked normal but had fewer cells (Figure 8h, d; see also Figure S9 for a close-up of the mature embryo RAM). The observed morphological defects are in agreement with marker line analyses. Expression of *DR5rev:GFP*, *pWOX:GFP*, and *pCLV3:GUS* was not strongly altered in *minu1 minu2* relative to wild-type torpedo or bent cotyledons stage embryos (Figure S10), but the number of cells expressing most markers was apparently reduced.

minu1-2 minu2-2 embryos displayed much more severe embryo development defects (Figure 8i–k). At the mid globular stage, *minu1-2 minu2-2* embryos had only reached the 1-cell stage of development (Figure 8i), the apical cell had not undergone any cell divisions, while the suspensor lineage had only achieved two cell divisions. At the mid heart stage, cells of the *minu1-2 minu2-2* embryo were enlarged, and the cell divisions were no longer merely delayed but also highly abnormal (Figure 8j). At the late torpedo stage, embryos of the strong allelic combination *minu1-2 minu2-2* showed a few additional disorganized cell divisions and seemed to have arrested their development (Figure 8k). Based on our morphological observations, none of the embryos initiated the stem cell populations of the SAM or RAM.

Developing *minu1-3 minu2-1* seed showed delayed greening compared to wild type (Figure 8l). Seed of the slightly stronger allelic combination *minu1-2 minu2-1* were more misshapen and developmentally delayed. The stronger (*minu1-3 minu2-2*) and strongest (*minu1-2 minu2-2*) allelic combinations triggered seed development arrest, resulting in white ovules (absence of a viable green embryo) that shriveled and dried out (Figure 8l).

DISCUSSION

Land plants have three types of SWI2/SNF2 subgroup chromatin remodeling ATPases; homologs of *Arabidopsis* BRAHMA, SPLAYED and MINU. Here we report that the MINU SWI2/SNF2 ATPases have important roles in development and that the two *MINU* genes present in *Arabidopsis* act redundantly. Like *syd* and *brm* single mutants (Farrona, *et al.* 2004, Wagner and Meyerowitz 2002), hypomorphic *minu1 minu2* double mutants displayed pleiotropic morphological defects. The activity of at least one MINU protein is required for embryo and endosperm development. Further, our studies point to a critical role for MINU1

or MINU2 in formation and maintenance of the stem cell population of the root and shoot apical meristem.

The post-embryonic phenotype of the shoot stem cell population in six-day-old *minu1 minu2* mutants resembles a loss-of-function *wus* phenotype (Mayer, *et al.* 1998). However, at this stage *minu1 minu2* meristems displayed increased expression of *WUS.* The increased expression of *WUS* is likely not the cause of the initial meristem defect as removal of WUS activity in *wus minu1 minu2* triple mutants did not lead to an improvement of the *minu1 minu2* SAM defect. In addition, at early developmental stages *minu1 minu2* shoot apices displayed a loss or reduction in *WUS* expression. The later increase in *WUS* expression may be a consequence of reduced WUS activity, as previously reported (Graf *et al.* 2010). We did not observe MINU2 recruitment to the *WUS* promoter by ChIP qPCR. MINU2 may be recruited to other regions of the *WUS* locus, for example to the 3′ intergenic region, which was recently implicated in recruitment of AGAMOUS and Polycomb repressors (Liu *et al.* 2011). Alternatively, MINU activity may indirectly affect *WUS* accumulation.

In the root, we observed reduced expression of the stem cell regulators *SHR* and *SCR*, particularly in the presumptive QC, which is consistent with a partial to full loss of QC identity as shown by a loss of the QC25 marker and misexpression of QC184 in the minu1 minu 2 root apices. In addition, the distal stem cells of the *minu1 minu2* root differentiated, a defect associated with loss of function of the WUS homolog *WOX5* (Sarkar, *et al.* 2007). Expression of p*WOX5:GFP* was increased and displaced proximally from the normal position of the QC in the *minu1 minu 2* roots. A similar expression defect is associated with a loss of WOX5 activity (Sarkar, *et al.* 2007). It is currently unclear whether *minu1 minu2* roots initially display a loss of *WOX5* expression in the QC that leads to the ectopic expression of *pWOX5:GFP* and divisions in the columella, or whether there is an uncoupling of *WOX5* expression and WOX5 function. MINU2 bound to the *WOX5* promoter, suggesting that MINU1/MINU2 can directly regulate *WOX5*.

We also observed reduced expression of cytokinin and auxin responsive genes in *minu1 minu2* mutant meristems as well as morphological defects reminiscent of mutations in cytokinin and/or auxin signaling pathways (Benkova *et al.* 2003, Brenner, *et al.* 2012, Buechel, *et al.* 2010, D'Agostino, *et al.* 2000, McSteen 2010, Reinhardt *et al.* 2003, Skylar, *et al.* 2010). Auxin and cytokinin hormone signaling plays important roles in meristem activity, particularly in the control of cell division (Buechel, *et al.* 2010, Friml, *et al.* 2003, Gordon, *et al.* 2009, Hardtke and Berleth 1998, Higuchi *et al.* 2004, Jasinski, *et al.* 2005, Kurakawa *et al.* 2007, Muller and Sheen 2008, Nishimura *et al.* 2004, Riefler *et al.* 2006, Skylar, *et al.* 2010, Tokunaga *et al.* 2012, Weijers, *et al.* 2006, Yanai, *et al.* 2005, Zhao *et al.* 2010). It is not clear whether MINU function directly impacts hormone responses, or whether the observed defects are an indirect consequence of the meristem defects.

The molecular and morphological defects of the *minu1 minu2* meristems are reminiscent of mutations in genes linked to replication-coupled chromatin assembly such as *FASCIATA1 (FAS1)* or *MGOUN3/TONOKU/BRUSHY1 (MGO3/TON/BRU1). FAS1* encodes the largest subunit of the Chromatin Assembly Factor1 (CAF1) complex, which is required for histone octamer deposition onto the newly replicated DNA (Kaya, *et al.* 2001, Smith and Stillman

1989). *MGO3/TON/BRU1* encodes a large protein containing tetratricopetide repeats, and LGN domains (Guyomarc'h *et al.* 2004, Ohno *et al.* 2011, Suzuki *et al.* 2004, Suzuki *et al.* 2005, Takeda, *et al.* 2004). LGN-domain containing proteins are implicated in asymmetric cell division in metazoans (Culurgioni *et al.* 2011, Matsumura *et al.* 2012, Yuzawa *et al.* 2011). *fas1* and *mgo/ton/bru* mutants cause loss of mitotic epigenetic memory, have short roots and display delayed leaf initiation (Kaya, *et al.* 2001, Suzuki, *et al.* 2004, Takeda, *et al.* 2004). In addition, *fas1* mutants enhance the shoot apical meristem defects of *wus* hypomorphic mutants (Graf, *et al.* 2010). *fas1* and *mgo/ton/bru* mutants delay mitotic progression and may lead to activation of the endocycle (Ramirez-Parra and Gutierrez 2007, Suzuki, *et al.* 2005). The similarities between *fas1, mgo3/ton/bru* and *minu1 minu2* mutants include defects in both the shoot and root apical meristems, altered phyllotaxy, ectopic foci of *WUS* expression that are highly variable between individuals, distal stem cell differentiation and defects in *SCR* expression, especially in the QC (Guyomarc'h, *et al.* 2004, Kaya, *et al.* 2001, Suzuki, *et al.* 2004, Takeda, *et al.* 2004, Vanstraelen *et al.* 2009). The endosperm defects of *minu1 minu2*: a reduction in the number and an increase in the size of the nuclei, are suggestive of reduced cell division and increased endoreduplication. However, while *minu1 minu2* mutants form multiple SAMs, these do not do fasciate like those of *fas1* or *mgo3/ton/bru1* mutants. The weaker phenotype may be due to the partial MINU activity in the *minu1 minu2* hypomorphs. In addition, *fas1* mutants do not display embryonic defects, while *mgo3/ton/bru1* and *minu1 minu2* mutants do. It is possible that other replication coupled chromatin assembly factors, such as ASF1, may act during embryo development in concert with MINU1 MINU2 and MGO3/TON/BRU1 (Kaya, *et al.* 2001).

There is precedent for a role of chromatin remodeling ATPases in mitotic epigenetic memory. Metazoan ISWI and CHD1chromatin remodeling ATPases have been linked to replication coupled chromatin assembly and hence epigenetic memory (Alabert and Groth 2012, Piatti *et al.* 2011). Moreover, a growing body of evidence has revealed important functions for SWI2/SNF2 subgroup ATPases in nuclear processes other than transcription, including DNA replication (Cohen *et al.* 2010, Euskirchen *et al.* 2011, Kim *et al.* 2012, Lee *et al.* 2010, Shaked *et al.* 2006, Tyagi *et al.* 2009, Zhao *et al.* 2009). Consistent with these considerations, we observed that the GFP-MINU2 protein associates with (late anaphase) mitotic chromosomes (Figure S11). We also noted striking similarities between partial loss of *MINU1 MINU2* function in the root and loss of CCS52A function. *CCS52A2* encodes an activator of the anaphase promoting complex/cyclosome (APC/C) linked to cell cycle progression (Vanstraelen, *et al.* 2009).

Future genetic and molecular assays are needed to determine what the direct targets of MINU activity are and whether there is a link between MINU1 and MINU2 and hormone signaling and/or mitotic inheritance of epigenetic memory. Such experiments will be most insightful if they make use of inducible cell type specific *minu1 minu2* double null mutants.

Experimental procedures

Plant material and growth conditions

All plants used were in Col background. Seeds were either sown on fertilized soil or plated on 1/2 MS medium (Sigma) containing 0.8% agar (or 1.5% agar for vertical plates) and 1%

sucrose, unless otherwise indicated. The sources for the plant lines used were as follows. Mutants: *minu1-2* (CS413977), *minu1-3* (SALK_015562), *minu2-1* (SALK_057856), *minu2-2* (CS904444); *Arabidopsis* Biological Resource Center (ABRC); *wus-1* and *clv3-7* (Fletcher, *et al.* 1999, Laux, *et al.* 1996), outcrossed to Col three times. Marker lines: *pWUS:GUS*, *pCLV3:GUS*, *pWOX5:GFP*, *pSCR:SCR-GFP*, *pSHR:SHR-GFP*, *DR5rev:GFP*, *pARR5:GUS*, *pARR7:GUS*, *QC184* and *QC25* (Baurle and Laux 2005, Blilou, *et al.* 2005, Brand, *et al.* 2002, D'Agostino, *et al.* 2000, Friml, *et al.* 2003, Gallagher, *et al.* 2004, Jeon, *et al.* 2010, Nakajima, *et al.* 2001). *minu1-3 minu2-1/+* plants homozygous for the marker lines were used for analysis. See supplementary information (Methods S1) for additional details on cloning and transgenic lines.

Phylogenetic analyses

SPLAYED (At2g28290), BRAHMA (At2g460200), MINU1 (At3g06010), and MINU2 (At5g19310) orthologous protein sequences were retrieved using PLAZA (http://bioinformatics.psb.ugent.be/plaza/) (Proost, *et al.* 2009) and imported into MacVector. Sequences were aligned using ClustalW. Neighbor-joining phylogenetic trees were created using bootstrapping and Poisson correct p-values.

Microscopy and imaging

β-glucuronidase (GUS) staining was as previously described (Gillmor *et al.* 2010, Pastore *et al.* 2011). Embryos were cleared in Hoyer's solution as previously described (Gillmor, *et al.* 2010).

Root cross-sections were prepared as described (Koizumi *et al.* 2011). GUS stained tissues were mounted in a drop of chloral hydrate solution (chloral hydrate:glycerol:water = 8 g:1 ml:2 ml) before imaging. To visualize starch granules in the columella root cap, a mixture of chloral hydrate and Lugol's solution (6:1) was used for mounting. GFP-MINU2 expression in the shoot was detected as previously described (Goldshmidt *et al.* 2008). Roots were stained with 0.01μg/ml propidium iodide (PI, Sigma), or 3 μM FM 4–64 dye (Invitrogen) for 5 minutes followed by brief rinsing with water. Confocal images were obtained using a Leica TCS SL microscope equipped with an argon-krypton ion laser with the appropriate filter sets.

Cell flux (F(x); cells per day) equals the root elongation during the period of measurement (V9(x)) divided by the length of the fully expanded cells (L(x)) F(x)=V(x)/L(x). To measure V(x), we marked the position of the root tip on the back of the Petri plate once per day to determine the root elongation rate on a given day. Length measurements were conduced after photocopying using imageJ. To measure L(x), we stained the root with 0.01 μg/ml propidium iodide (PI, Sigma) to image the cortical cells. We measured the length of 10~20 cortical cells per root in the region of the maturation zone where root hair length was roughly half maximal. This region is comprised of cells that have just exited the cell expansion zone.

RNA analysis

For semi-quantitative and quantitative RT-PCR, total RNA was extracted from 3-day-old whole seedlings or dissected 6-day-old shoots or roots (Yamaguchi, *et al.* 2009). RNA levels were normalized to those *UBQ10* (At4g05320). Primers are listed in Table S4. In situ hybridization was performed as previously described (Wu, *et al.* 2012).

Chromatin immunoprecipitation(ChIP)

Chip was performed as previously described (Winter *et al.* 2011) using the primers listed in Table S4.

Supplementary Material

Refer to Web version on PubMed Central for supplementary material.

Acknowledgments

We thank Jennifer Fletcher for *clv3-7* and *wus-1* seeds, Ben Scheres for *pWOX5:GFP*, *QC184* and *QC25* seeds, Rüdiger Simon for *pCLV3:GUS* seeds, Joe Kieber for *pARR5:GUS*, Jungmook Kim for *pARR7:GUS*, and Thomas Laux for the *pWUS:GUS* binary construct. C.S.G. thanks Jean-Philippe Vielle-Calzada for Nomarski microscope use. This research was supported by institutional funds from CINVESTAV-IPN to C.S.G., and NIH grant R01 GM64650-01 to D.W.. S. W. was partially supported by NSF grant 0920327 awarded to K.L.G.; Y.S., N.Y., and M-F. W. were partially supported by NSF grant IOS-0849298 to D.W. J.P was supported by NRSA F32-GM076933.

References

Aichinger E, et al. The CHD3 chromatin remodeler PICKLE and polycomb group proteins antagonistically regulate meristem activity in the Arabidopsis root. The Plant cell. 2011; 23:1047–1060. [PubMed: 21441433]

Aida M, et al. The PLETHORA genes mediate patterning of the Arabidopsis root stem cell niche. Cell. 2004; 119:109–120. [PubMed: 15454085]

Alabert C, Groth A. Chromatin replication and epigenome maintenance. Nature reviews Molecular cell biology. 2012; 13:153–167.

Barrero JM, et al. INCURVATA2 encodes the catalytic subunit of DNA Polymerase alpha and interacts with genes involved in chromatin-mediated cellular memory in Arabidopsis thaliana. The Plant cell. 2007; 19:2822–2838. [PubMed: 17873092]

Barton K, Poethig RS. Formation of the shoot apical meristem in Arabidopsis thaliana: an analysis of development in the wild type and in the shoot meristemless mutant. Development. 1993; 119:823–831.

Baurle I, Laux T. Regulation of WUSCHEL transcription in the stem cell niche of the Arabidopsis shoot meristem. The Plant cell. 2005; 17:2271–2280. [PubMed: 15980263]

Beemster GT, Baskin TI. Analysis of cell division and elongation underlying the developmental acceleration of root growth in Arabidopsis thaliana. Plant physiology. 1998; 116:1515–1526. [PubMed: 9536070]

Benkova E, et al. Local, efflux-dependent auxin gradients as a common module for plant organ formation. Cell. 2003; 115:591–602. [PubMed: 14651850]

Bezhani S, et al. Unique, shared, and redundant roles for the Arabidopsis SWI/SNF chromatin remodeling ATPases BRAHMA and SPLAYED. Plant Cell. 2007; 19:403–416. [PubMed: 17293567]

Blilou I, et al. The PIN auxin efflux facilitator network controls growth and patterning in Arabidopsis roots. Nature. 2005; 433:39–44. [PubMed: 15635403]

Brand U, et al. Dependence of stem cell fate in Arabidopsis on a feedback loop regulated by CLV3 activity. Science. 2000; 289:617–619. [PubMed: 10915624]

Brand U, et al. Regulation of CLV3 expression by two homeobox genes in Arabidopsis. Plant Physiol. 2002; 129:565–575. [PubMed: 12068101]

Brenner M, et al. Gene regulation by cytokinin in Arabidopsis. Front Plant Sci. 2012; 3(8)10.3389/fpls.2012.00008

Buechel S, et al. Role of A-type ARABIDOPSIS RESPONSE REGULATORS in meristem maintenance and regeneration. European journal of cell biology. 2010; 89:279–284. [PubMed: 20018401]

Clapier CR, Cairns BR. The biology of chromatin remodeling complexes. Annu Rev Biochem. 2009; 78:273–304. [PubMed: 19355820]

Clark SE, et al. The CLAVATA and SHOOT MERISTEMLESS loci competitively regulate meristem activity in Arabidopsis. Development. 1996; 122:1567–1575. [PubMed: 8625843]

Cohen SM, et al. BRG1 co-localizes with DNA replication factors and is required for efficient replication fork progression. Nucleic Acids Res. 2010; 38:6906–6919. [PubMed: 20571081]

Colon-Carmona A, et al. Technical advance: spatio-temporal analysis of mitotic activity with a labilecyclin-GUS fusion protein. The Plant journal: for cell and molecular biology. 1999; 20:503–508. [PubMed: 10607302]

Culurgioni S, et al. Inscuteable and NuMA proteins bind competitively to Leu-Gly-Asn repeat-enriched protein (LGN) during asymmetric cell divisions. Proceedings of the National Academy of Sciences of the United States of America. 2011; 108:20998–21003. [PubMed: 22171003]

D'Agostino IB, et al. Characterization of the response of the Arabidopsis response regulator gene family to cytokinin. Plant physiology. 2000; 124:1706–1717. [PubMed: 11115887]

Euskirchen GM, et al. Diverse roles and interactions of the SWI/SNF chromatin remodeling complex revealed using global approaches. PLoS genetics. 2011; 7:e1002008. [PubMed: 21408204]

Farrona S, et al. The Arabidopsis thaliana SNF2 homolog AtBRM controls shoot development and flowering. Development. 2004; 131:4965–4975. [PubMed: 15371304]

Farrona S, et al. Brahma is required for proper expression of the floral repressor FLC in Arabidopsis. PloS one. 2011; 6:e17997. [PubMed: 21445315]

Farrona S, et al. A nucleosome interaction module is required for normal function of Arabidopsis thaliana BRAHMA. J Mol Biol. 2007; 373:240–250. [PubMed: 17825834]

Flaus A, et al. Identification of multiple distinct Snf2 subfamilies with conserved structural motifs. Nucleic Acids Res. 2006; 34:2887–2905. [PubMed: 16738128]

Flaus A, Owen-Hughes T. Mechanisms for ATP-dependent chromatin remodelling: the means to the end. Febs J. 2011; 278:3579–3595. [PubMed: 21810178]

Fletcher JC, et al. Signaling of cell fate decisions by CLAVATA3 in Arabidopsis shoot meristems. Science. 1999; 283:1911–1914. [PubMed: 10082464]

Friml J, et al. Efflux-dependent auxin gradients establish the apical-basal axis of Arabidopsis. Nature. 2003; 426:147–153. [PubMed: 14614497]

Galinha C, et al. PLETHORA proteins as dose-dependent master regulators of Arabidopsis root development. Nature. 2007; 449:1053–1057. [PubMed: 17960244]

Gallagher KL, et al. Mechanisms regulating SHORT-ROOT intercellular movement. Current biology: CB. 2004; 14:1847–1851. [PubMed: 15498493]

Gillmor CS, et al. The MED12-MED13 module of Mediator regulates the timing of embryo patterning in Arabidopsis. Development. 2010; 137:113–122. [PubMed: 20023166]

Goldshmidt A, et al. Signals derived from YABBY gene activities in organ primordia regulate growth and partitioning of Arabidopsis shoot apical meristems. The Plant cell. 2008; 20:1217–1230. [PubMed: 18469164]

Gordon SP, et al. Multiple feedback loops through cytokinin signaling control stem cell number within the Arabidopsis shoot meristem. Proceedings of the National Academy of Sciences of the United States of America. 2009; 106:16529–16534. [PubMed: 19717465]

Graf P, et al. MGOUN1 encodes an Arabidopsis type IB DNA topoisomerase required in stem cell regulation and to maintain developmentally regulated gene silencing. The Plant cell. 2010; 22:716–728. [PubMed: 20228247]

Guyomarc'h S, et al. MGOUN3, an Arabidopsis gene with TetratricoPeptide-Repeat-related motifs, regulates meristem cellular organization. Journal of experimental botany. 2004; 55:673–684. [PubMed: 14966212]

Hardtke CS, Berleth T. The Arabidopsis gene MONOPTEROS encodes a transcription factor mediating embryo axis formation and vascular development. The EMBO journal. 1998; 17:1405–1411. [PubMed: 9482737]

Helariutta Y, et al. The SHORT-ROOT gene controls radial patterning of the Arabidopsis root through radial signaling. Cell. 2000; 101:555–567. [PubMed: 10850497]

Higuchi M, et al. In planta functions of the Arabidopsis cytokinin receptor family. Proceedings of the National Academy of Sciences of the United States of America. 2004; 101:8821–8826. [PubMed: 15166290]

Ho L, et al. An embryonic stem cell chromatin remodeling complex, esBAF, is an essential component of the core pluripotency transcriptional network. Proc Natl Acad Sci U S A. 2009; 106:5187–5191. [PubMed: 19279218]

Hurtado L, et al. The putative SWI/SNF complex subunit BRAHMA activates flower homeotic genes in Arabidopsis thaliana. Plant Mol Biol. 2006

Jasinski S, et al. KNOX action in Arabidopsis is mediated by coordinate regulation of cytokinin and gibberellin activities. Current biology: CB. 2005; 15:1560–1565. [PubMed: 16139211]

Jeon J, et al. A subset of cytokinin two-component signaling system plays a role in cold temperature stress response in Arabidopsis. The Journal of biological chemistry. 2010; 285:23371–23386. [PubMed: 20463025]

Jerzmanowski A. SWI/SNF chromatin remodeling and linker histones in plants. Biochim Biophys Acta. 2007; 1769:330–345. [PubMed: 17292979]

Kaya H, et al. FASCIATA genes for chromatin assembly factor-1 in arabidopsis maintain the cellular organization of apical meristems. Cell. 2001; 104:131–142. [PubMed: 11163246]

Kim Y, et al. An essential role for a mammalian SWI/SNF chromatin-remodeling complex during male meiosis. Development. 2012

Koizumi K, et al. An essential protein that interacts with endosomes and promotes movement of the SHORT-ROOT transcription factor. Current biology: CB. 2011; 21:1559–1564. [PubMed: 21924907]

Kornet N, Scheres B. Members of the GCN5 histone acetyltransferase complex regulate PLETHORA-mediated root stem cell niche maintenance and transit amplifying cell proliferation in Arabidopsis. The Plant cell. 2009; 21:1070–1079. [PubMed: 19376933]

Kurakawa T, et al. Direct control of shoot meristem activity by a cytokinin-activating enzyme. Nature. 2007; 445:652–655. [PubMed: 17287810]

Kwon CS, et al. WUSCHEL is a primary target for transcriptional regulation by SPLAYED in dynamic control of stem cell fate in Arabidopsis. Genes Dev. 2005; 19:992–1003. [PubMed: 15833920]

Kwon CS, et al. A role for chromatin remodeling in regulation of CUC gene expression in the Arabidopsis cotyledon boundary. Development. 2006; 133:3223–3230. [PubMed: 16854978]

Laux T, et al. The WUSCHEL gene is required for shoot and floral meristem integrity in Arabidopsis. Development. 1996; 122:87–96. [PubMed: 8565856]

Lee HS, et al. A cooperative activation loop among SWI/SNF, gamma-H2AX and H3 acetylation for DNA double-strand break repair. Embo J. 2010; 29:1434–1445. [PubMed: 20224553]

Leibfried A, et al. WUSCHEL controls meristem function by direct regulation of cytokinin-inducible response regulators. Nature. 2005; 438:1172–1175. [PubMed: 16372013]

Lenhard M, et al. The WUSCHEL and SHOOTMERISTEMLESS genes fulfil complementary roles in Arabidopsis shoot meristem regulation. Development. 2002; 129:3195–3206. [PubMed: 12070094]

Liu X, et al. AGAMOUS terminates floral stem cell maintenance in Arabidopsis by directly repressing WUSCHEL through recruitment of Polycomb Group proteins. Plant Cell. 2011; 23:3654–3670. [PubMed: 22028461]

Long J, Barton MK. Initiation of axillary and floral meristems in Arabidopsis. Dev Biol. 2000; 218:341–353. [PubMed: 10656774]

Long JA, et al. A member of the KNOTTED class of homeodomain proteins encoded by the STM gene of Arabidopsis. Nature. 1996; 379:66–69. [PubMed: 8538741]

Matsumura S, et al. ABL1 regulates spindle orientation in adherent cells and mammalian skin. Nat Commun. 2012; 3:626. [PubMed: 22252550]

Mayer KF, et al. Role of WUSCHEL in regulating stem cell fate in the Arabidopsis shoot meristem. Cell. 1998; 95:805–815. [PubMed: 9865698]

McSteen P. Auxin and monocot development. Cold Spring Harb Perspect Biol. 2010; 2:a001479. [PubMed: 20300208]

Mlynarova L, et al. The SWI/SNF chromatin-remodeling gene AtCHR12 mediates temporary growth arrest in Arabidopsis thaliana upon perceiving environmental stress. Plant J. 2007; 51:874–885. [PubMed: 17605754]

Muller B, Sheen J. Cytokinin and auxin interaction in root stem-cell specification during early embryogenesis. Nature. 2008; 453:1094–1097. [PubMed: 18463635]

Nakajima K, et al. Intercellular movement of the putative transcription factor SHR in root patterning. Nature. 2001; 413:307–311. [PubMed: 11565032]

Nishimura C, et al. Histidine kinase homologs that act as cytokinin receptors possess overlapping functions in the regulation of shoot and root growth in Arabidopsis. The Plant cell. 2004; 16:1365–1377. [PubMed: 15155880]

Ohno Y, et al. Ectopic gene expression and organogenesis in Arabidopsis mutants missing BRU1 required for genome maintenance. Genetics. 2011; 189:83–95. [PubMed: 21705754]

Ori N, et al. Mechanisms that control knox gene expression in the Arabidopsis shoot. Development. 2000; 127:5523–5532. [PubMed: 11076771]

Pastore JJ, et al. LATE MERISTEM IDENTITY2 acts together with LEAFY to activate APETALA1. Development. 2011; 138:3189–3198. [PubMed: 21750030]

Phelps-Durr TL, et al. Maize rough sheath2 and its Arabidopsis orthologue ASYMMETRIC LEAVES1 interact with HIRA, a predicted histone chaperone, to maintain knox gene silencing and determinacy during organogenesis. The Plant cell. 2005; 17:2886–2898. [PubMed: 16243907]

Piatti P, et al. ATP-Dependent Chromatin Remodeling Factors and Their Roles in Affecting Nucleosome Fiber Composition. Int J Mol Sci. 2011; 12:6544–6565. [PubMed: 22072904]

Proost S, et al. PLAZA: a comparative genomics resource to study gene and genome evolution in plants. The Plant cell. 2009; 21:3718–3731. [PubMed: 20040540]

Ramirez-Parra E, Gutierrez C. E2F regulates FASCIATA1, a chromatin assembly gene whose loss switches on the endocycle and activates gene expression by changing the epigenetic status. Plant physiology. 2007; 144:105–120. [PubMed: 17351056]

Reinhardt D, et al. Regulation of phyllotaxis by polar auxin transport. Nature. 2003; 426:255–260. [PubMed: 14628043]

Riefler M, et al. Arabidopsis cytokinin receptor mutants reveal functions in shoot growth, leaf senescence, seed size, germination, root development, and cytokinin metabolism. The Plant cell. 2006; 18:40–54. [PubMed: 16361392]

Sabatini S, et al. SCARECROW is involved in positioning the stem cell niche in the Arabidopsis root meristem. Genes & development. 2003; 17:354–358. [PubMed: 12569126]

Sarkar AK, et al. Conserved factors regulate signalling in Arabidopsis thaliana shoot and root stem cell organizers. Nature. 2007; 446:811–814. [PubMed: 17429400]

Schoof H, et al. The stem cell population of Arabidopsis shoot meristems in maintained by a regulatory loop between the CLAVATA and WUSCHEL genes. Cell. 2000; 100:635–644. [PubMed: 10761929]

Schubert D, et al. Silencing by plant Polycomb-group genes requires dispersed trimethylation of histone H3 at lysine 27. Embo J. 2006; 25:4638–4649. [PubMed: 16957776]

Shaked H, et al. Involvement of the Arabidopsis SWI2/SNF2 chromatin remodeling gene family in DNA damage response and recombination. Genetics. 2006; 173:985–994. [PubMed: 16547115]

Skylar A, et al. STIMPY mediates cytokinin signaling during shoot meristem establishment in Arabidopsis seedlings. Development. 2010; 137:541–549. [PubMed: 20110319]

Smith S, Stillman B. Purification and characterization of CAF-I, a human cell factor required for chromatin assembly during DNA replication in vitro. Cell. 1989; 58:15–25. [PubMed: 2546672]

Suzuki T, et al. A novel Arabidopsis gene TONSOKU is required for proper cell arrangement in root and shoot apical meristems. The Plant journal: for cell and molecular biology. 2004; 38:673–684. [PubMed: 15125773]

Suzuki T, et al. TONSOKU is expressed in S phase of the cell cycle and its defect delays cell cycle progression in Arabidopsis. Plant & cell physiology. 2005; 46:736–742. [PubMed: 15746155]

Takeda S, et al. BRU1, a novel link between responses to DNA damage and epigenetic gene silencing in Arabidopsis. Genes & development. 2004; 18:782–793. [PubMed: 15082530]

Tamkun JW, et al. brahma: a regulator of Drosophila homeotic genes structurally related to the yeast transcriptional activator SNF2/SWI2. Cell. 1992; 68:561–572. [PubMed: 1346755]

Tang X, et al. The Arabidopsis BRAHMA chromatin-remodeling ATPase is involved in repression of seed maturation genes in leaves. Plant Physiol. 2008; 147:1143–1157. [PubMed: 18508955]

Tokunaga H, et al. Arabidopsis lonely guy (LOG) multiple mutants reveal a central role of the LOG-dependent pathway in cytokinin activation. The Plant journal: for cell and molecular biology. 2012; 69:355–365. [PubMed: 22059596]

Tyagi A, et al. SWI/SNF associates with nascent pre-mRNPs and regulates alternative pre-mRNA processing. PLoS Genet. 2009; 5:e1000470. [PubMed: 19424417]

Vandepoele K, et al. Genome-wide analysis of core cell cycle genes in Arabidopsis. The Plant cell. 2002; 14:903–916. [PubMed: 11971144]

Vanstraelen M, et al. APC/C-CCS52A complexes control meristem maintenance in the Arabidopsis root. Proceedings of the National Academy of Sciences of the United States of America. 2009; 106:11806–11811. [PubMed: 19553203]

Wagner D, Meyerowitz EM. SPLAYED, a novel SWI/SNF ATPase homolog, controls reproductive development in Arabidopsis. Curr Biol. 2002; 12:85–94. [PubMed: 11818058]

Weijers D, et al. Auxin triggers transient local signaling for cell specification in Arabidopsis embryogenesis. Developmental cell. 2006; 10:265–270. [PubMed: 16459305]

Winter CM, et al. LEAFY Target Genes Reveal Floral Regulatory Logic, cis Motifs, and a Link to Biotic Stimulus Response. Developmental cell. 2011; 20:430–443. [PubMed: 21497757]

Wu MF, et al. SWI2/SNF2 chromatin remodeling ATPases overcome polycomb repression and control floral organ identity with the LEAFY and SEPALLATA3 transcription factors. Proceedings of the National Academy of Sciences of the United States of America. 2012; 109:3576–3581. [PubMed: 22323601]

Xu L, Shen WH. Polycomb silencing of KNOX genes confines shoot stem cell niches in Arabidopsis. Current biology: CB. 2008; 18:1966–1971. [PubMed: 19097900]

Yamaguchi A, et al. The microRNA-regulated SBP-Box transcription factor SPL3 is a direct upstream activator of LEAFY, FRUITFULL, and APETALA1. Developmental cell. 2009; 17:268–278. [PubMed: 19686687]

Yanai O, et al. Arabidopsis KNOXI proteins activate cytokinin biosynthesis. Current biology: CB. 2005; 15:1566–1571. [PubMed: 16139212]

Yuzawa S, et al. Structural basis for interaction between the conserved cell polarity proteins Inscuteable and Leu-Gly-Asn repeat-enriched protein (LGN). Proceedings of the National Academy of Sciences of the United States of America. 2011; 108:19210–19215. [PubMed: 22074847]

Zhao Q, et al. Modulation of nucleotide excision repair by mammalian SWI/SNF chromatin-remodeling complex. J Biol Chem. 2009; 284:30424–30432. [PubMed: 19740755]

Zhao Z, et al. Hormonal control of the shoot stem-cell niche. Nature. 2010; 465:1089–1092. [PubMed: 20577215]

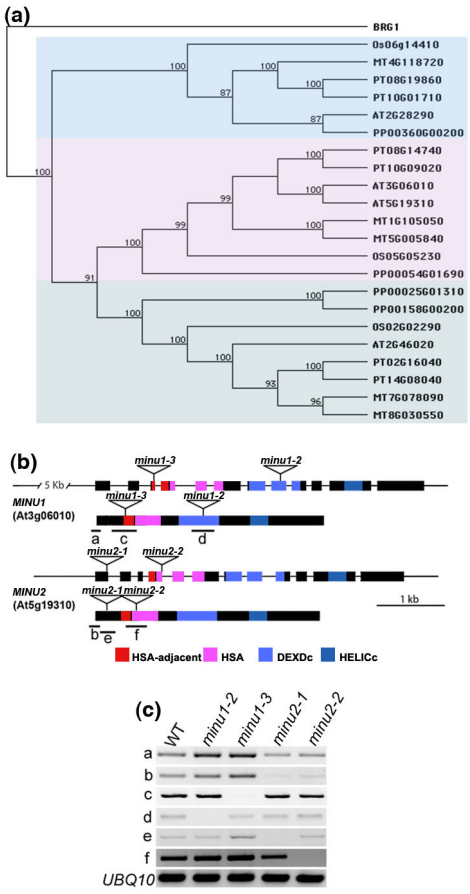

Figure 1. Identification of *minu1* and *minu2* mutant alleles

(a) Phylogenetic analysis of MINU1 and MINU2 orthologs in select tracheophytes (see also Figure S1). The human SWI2/SNF2 ATPase Brg1 was included as the outgroup. AT: *Arabidopsis thaliana*; OS: *Oryza sativa*; MT: *Medicago trunculata*; PT: *Populus trichocarpa*; PP: *Physcomitrella patens.* Bootstrap values: % invariant branches during resampling. (b) Schematic of the *MINU1* and *MINU2* loci and mRNAs. Boxes and lines indicate coding and non-coding regions, respectively. Regions encoding for known protein domains are color-coded and were identified using online tools (http://smart.embl-heidelberg.de/). Triangles: T-DNA insertion sites. (c) *MINU1* and *MINU2* mRNA levels based on semi-quantitative RT-PCR from three-day-old seedlings. Top: genotype; left: amplicon (see (b) for approximate position). *UBQ10* (At4g05320) served as internal control.

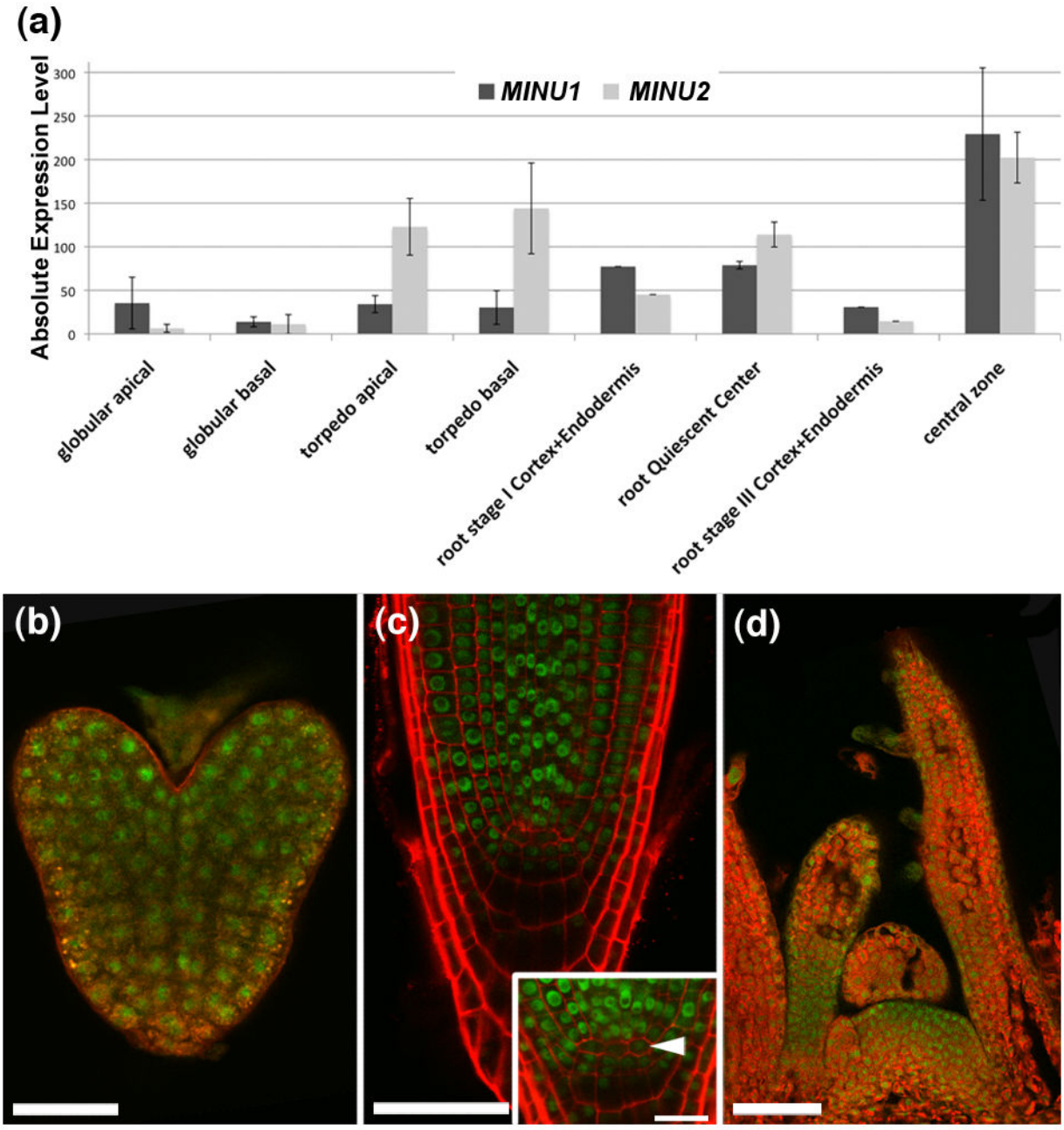

Figure 2. MINU2 is nuclear localized and expressed in rapidly dividing cells

(a) *MINU1* and *MINU2* mRNA expression levels in select tissues. Data were extracted from public expression arrays (http://bar.utoronto.ca/efp/cgi-bin/efpWeb.cgi). Mean ± SEM are shown. (b–d) Expression of GFP-MINU2 protein in *minu1-2 minu2-1* plants at different developmental stages: heart stage embryo (b), five-day-old root tip (c) and fifteen-day-old shoot apex (d). Bars = 50 μm (b and c), or 20 μm (d). Inset in (c): higher magnification view of the QC (arrowhead). Bar = 20 μm.

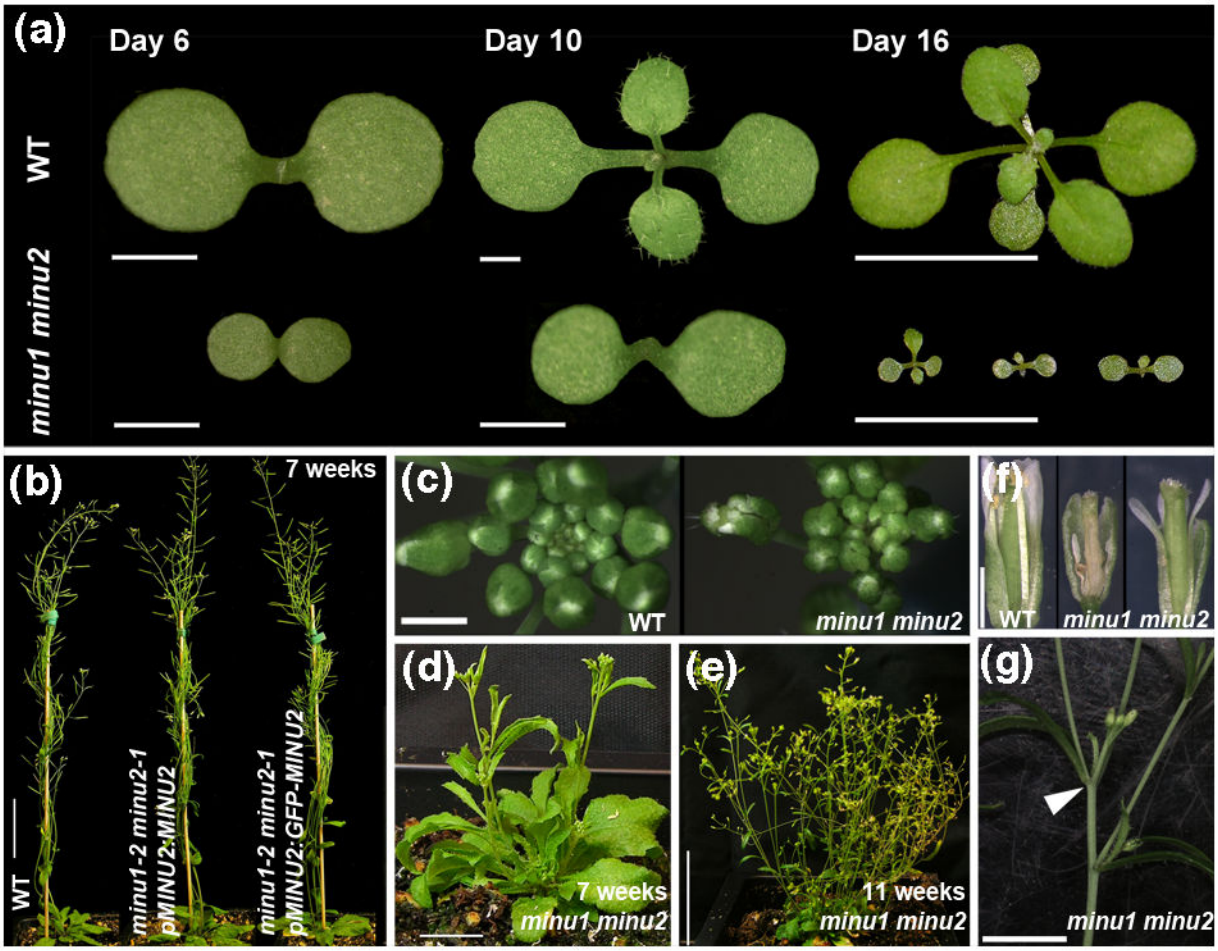

Figure 3. Post-embryonic defects of *minu1 minu2* aerial tissues

(a) Top view of soil-grown wild-type (WT) and *minu1 minu2* plants at indicated time points (above). Bars = 1 mm (Day 6 and 10) or 1 cm (Day 16). (b) Seven-week-old wild-type (WT) and *minu1-2 minu2-1* plants expressing untagged or GFP-tagged MINU2. Bar = 5 cm. (c) Top view of ~5 cm bolt of wild-type and *minu1 minu2* inflorescences. Bar = 1 mm. (d) Seven-week-old *minu1 minu2* plant. Bar = 1 cm. (e) Eleven-week-old *minu1 minu2* plant. Bar = 5 cm. (f) Early (middle) and late (right) arising flowers of *minu1 minu2* plants and representative wild-type flower (WT). Some outer organs were removed to reveal inner whorls. Bar = 1 mm. (g) Altered phyllotaxy in *minu1 minu2* plants. Three inflorescence stems originated from one node (arrowhead). Bar = 1 cm.

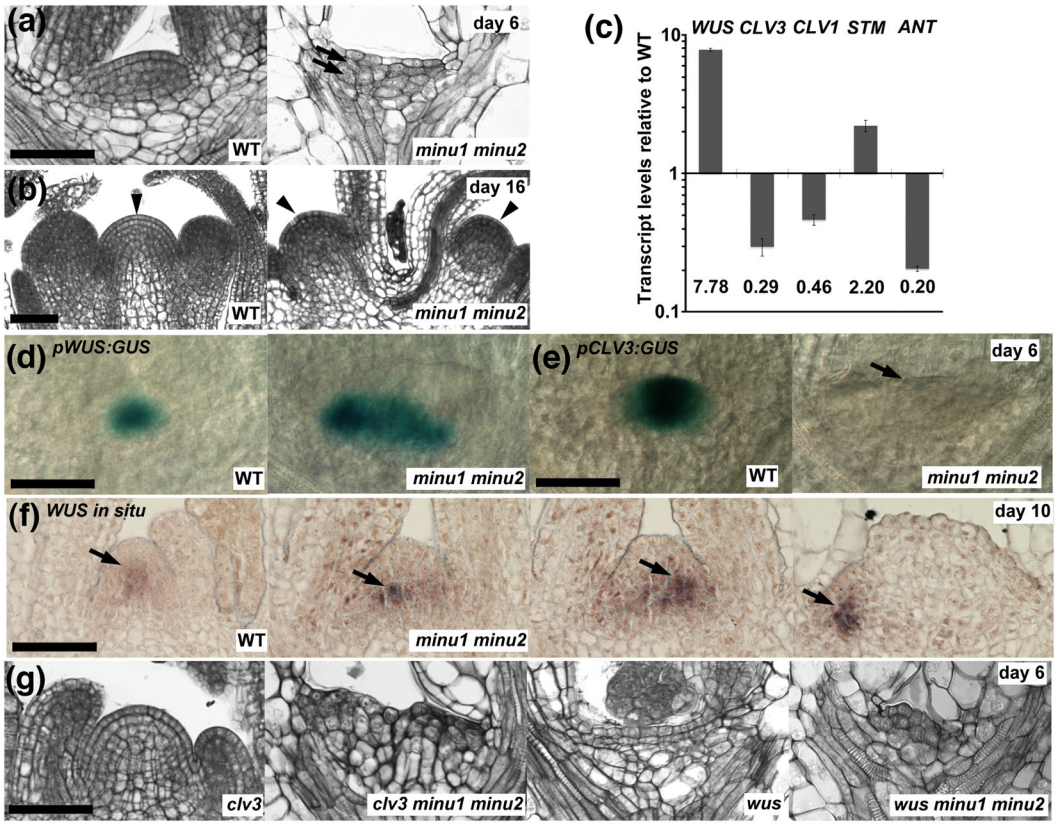

Figure 4. Molecular defects of *minu1 minu2* SAMs

(a–b) Longitudinal sections of wild-type (WT) and *minu1 minu2* SAMs as labeled. Arrows in (a): periclinal divisions. Arrowheads in (b): SAMs. (c) Transcript levels of markers of stem cell identity and differentiation in six-day-old shoot apices of *minu1 minu2* relative to the wild type based on quantitative RT-PCR. Shown are mean ± SEM of three technical replicates from one representative biological replicate. (d, e) Whole-mount images of *pWUS:GUS* (d) and *pCLV3:GUS* (e) expression in wild-type (WT) and *minu1 minu2* SAMs. Arrow in (e): weak GUS expression. (f) *WUS in situ* hybridization in a ten-day-old wild-type (WT) SAMs and in three sections from a single *minu1 minu2* SAM. Arrows indicate the *WUS* expression foci. (g) Longitudinal sections of SAMs from six-day-old plants of the genotypes indicated. All bars = 50 μm.

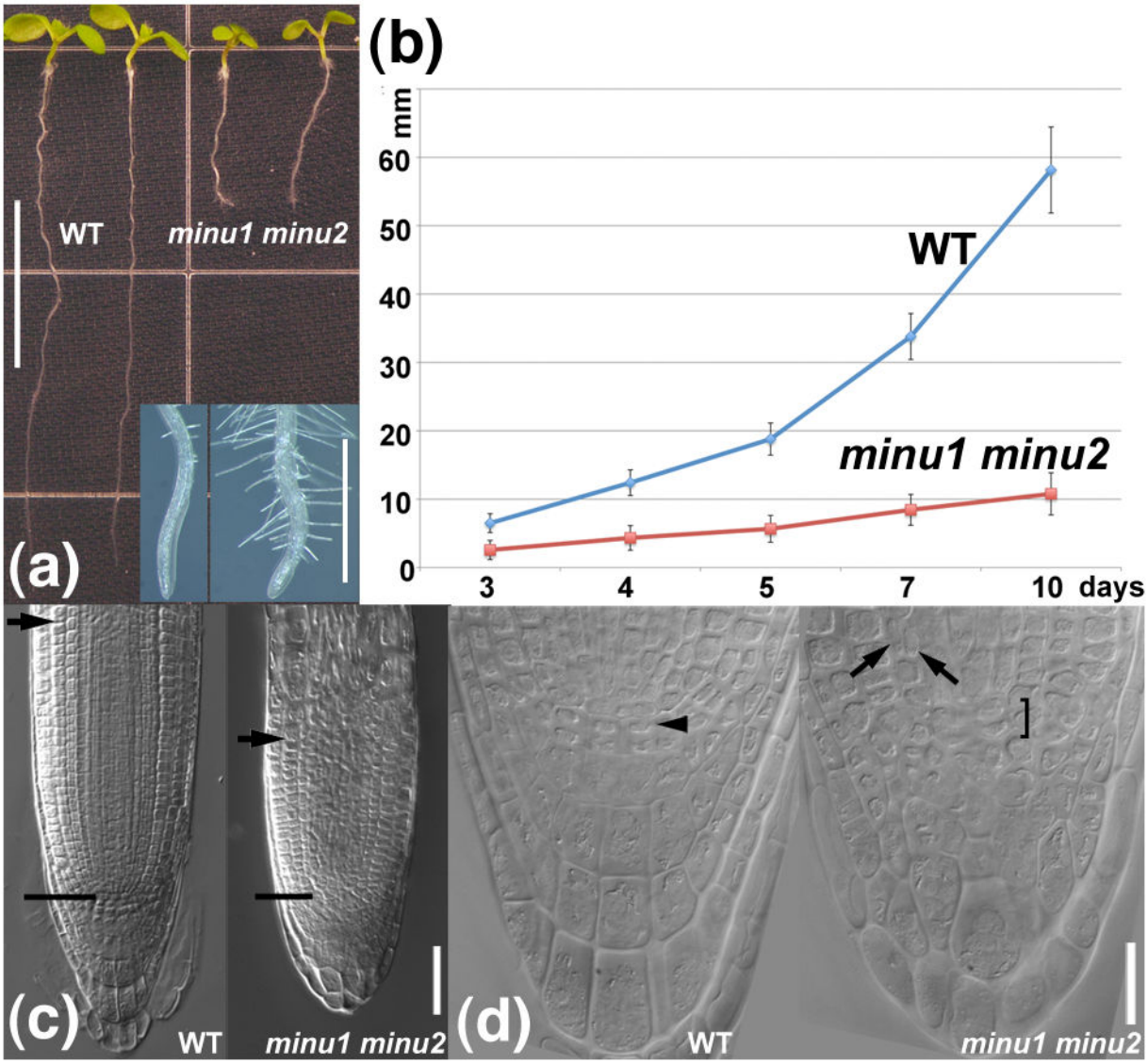

Figure 5. Post-embryonic defects of *minu1 minu2* root meristems

(a) Seven-day-old wild-type (WT) and *minu1 minu2* seedlings. Bar = 1cm. Inset shows a close-up of four-day-old root tips of WT (left) and *minu1 minu2* (right). Bar = 1 mm. (b) Root growth in WT (n=119) and *minu1 minu2* (n=21) plants. (c) Root meristem size of five-day-old wild-type (WT) and *minu1 minu2* plants. Lines: QC regions, arrows: transition from the meristematic to the elongation zone. Bar = 50 μm. (d) DIC images showing RAM organization in five-day-old wild type (WT) and *minu1 minu2*. Bar = 20 μm. Arrowhead: QC in the wild type, bracket: QC region in the *minu1 minu2* mutant, arrows: periclinal division in endodermis.

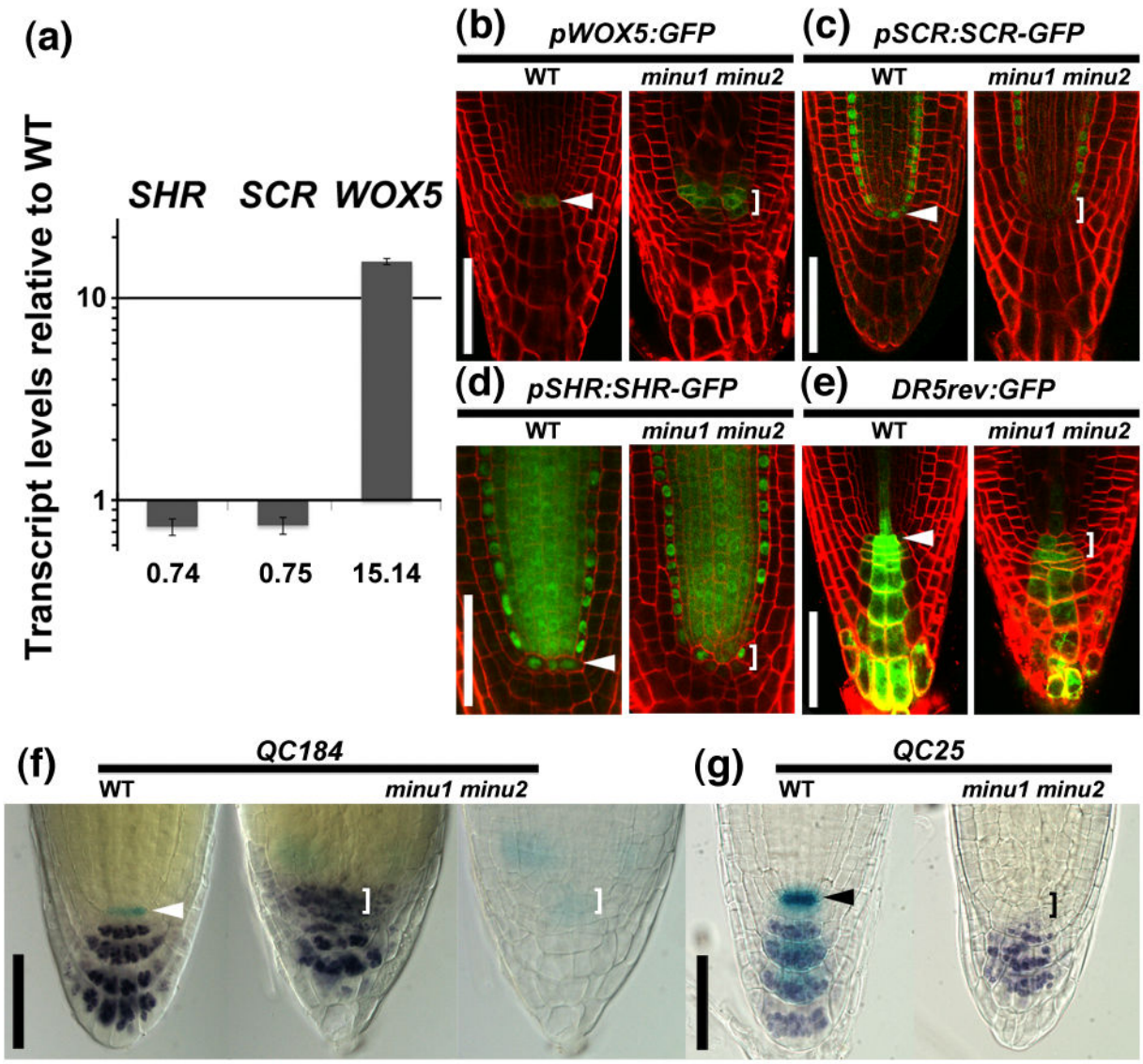

Figure 6. Molecular defects of *minu1 minu2* RAMs

(a) Transcript levels of meristem markers in six-day-old *minu1 minu2* root apices relative to those of the wildtype as determined by quantitative RT-PCR. Shown are mean ± SEM of three technical replicates from one representative biological replicate. (b–e) Reporter expression (as indicated) in five-day-old wild type (WT) or *minu1 minu2* RAMs. In wildtype, *pWOX5:GFP* (b) marks the QC; *pSCR:SCR-GFP* (c) marks the endodermis and QC and *pSHR:SHR-GFP* (d) marks the stele, endodermis and QC; *DR5rev:GFP* (e) is expressed in the columella root cap and initials, in the QC and in the innermost stele cells. (f, g) Visualization of the GUS-tagged (blue) QC markers *QC184* (f) and *QC25* (g) in wild-type (WT) and *minu1 minu2* plants. Plants were also stained with iodine to visualize starch deposits in the differentiated columella root cap cells (purple). The rightmost plant in (f) is identical to the center plant but re-photographed after loss of the transient starch staining. Arrowheads: QC in the wild type, bracket: presumptive QC region in *minu1 minu2*. All bars = 50 μm.

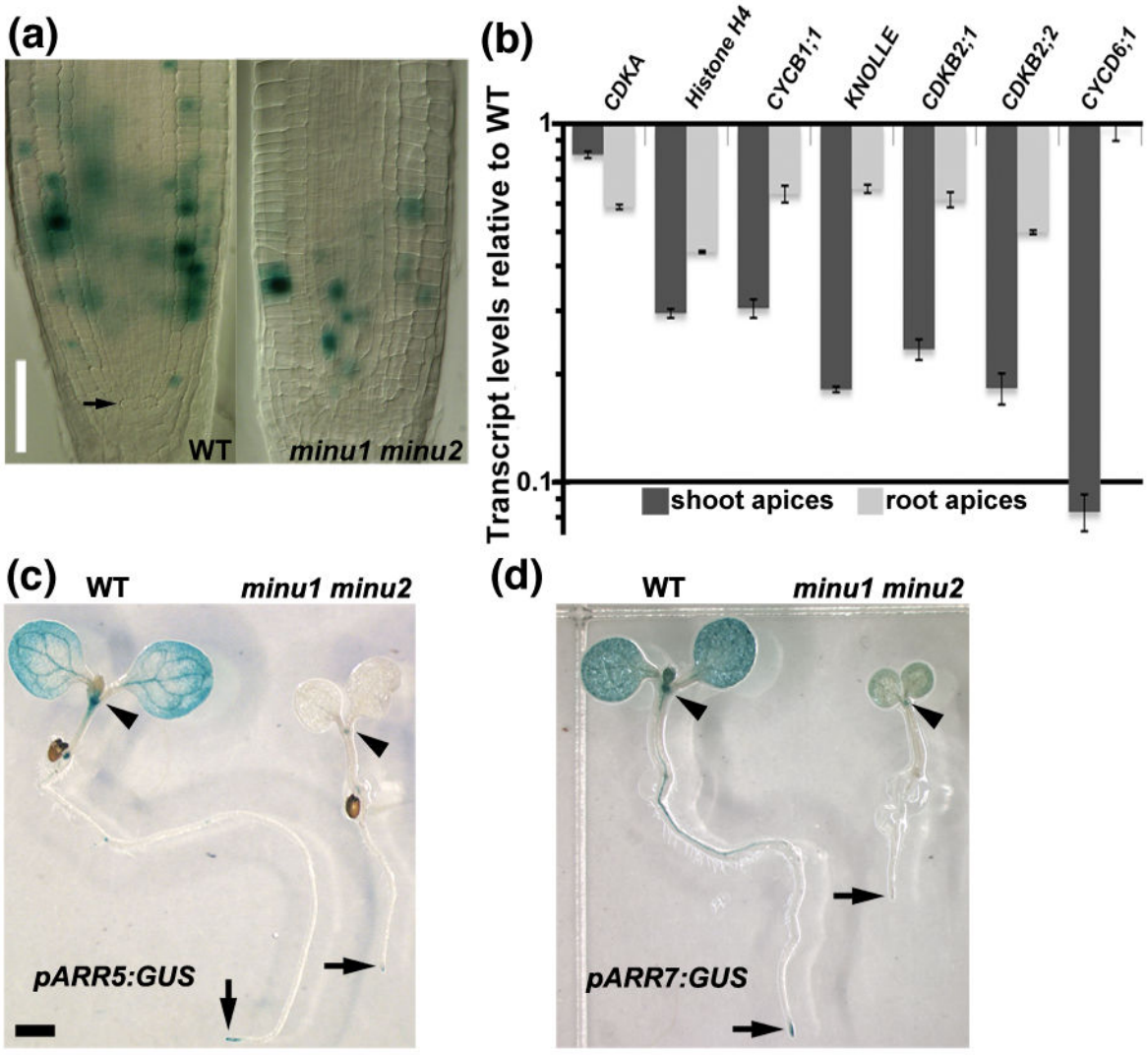

Figure 7. Reduced cell proliferation in *minu1 minu2* SAMs and RAMs

(a) Expression of *pCYCB1;1:CYCB1;1-GUS* in six-day-old wild-type (WT) and *minu1 minu2* roots. Bar = 50 μm. Arrow in (a) indicates the position of QC cells. (b) Transcript levels of cell-cycle regulator genes in six-day-old *minu1 minu2* shoot and root apices, determined by quantitative RT-PCR. Shown is the fold change of the expression in *minu1 minu2* over that of the wild type. The mean ± SEM of three technical replicates from one representative biological sample are indicated. *CDKA* is a general regulator of cell cycle progression whose activity peaks at the G1/S and G2/M transitions; *Histone H4* and *KNOLLE* are specifically expressed in S- and M-phase, respectively; *CYCB1;1* is a mitotic cyclin required for G2/M transition of the cell cycle and expressed in all actively dividing tissues; *CDKB2;1* and *CDKB2;2* are expressed at the G2/M boundary; *CYCD6;1* is a positive regulator of S-phase entry (Vandepoele *et al.* 2002). (c, d) Expression of two cytokinin response reporters, *pARR5:GUS* (c) and *pARR7:GUS* (d) in six-day-old wild-type and *minu1 minu2* seedling. Arrowhead: SAMs, arrows: RAMs. Bar = 1 mm.

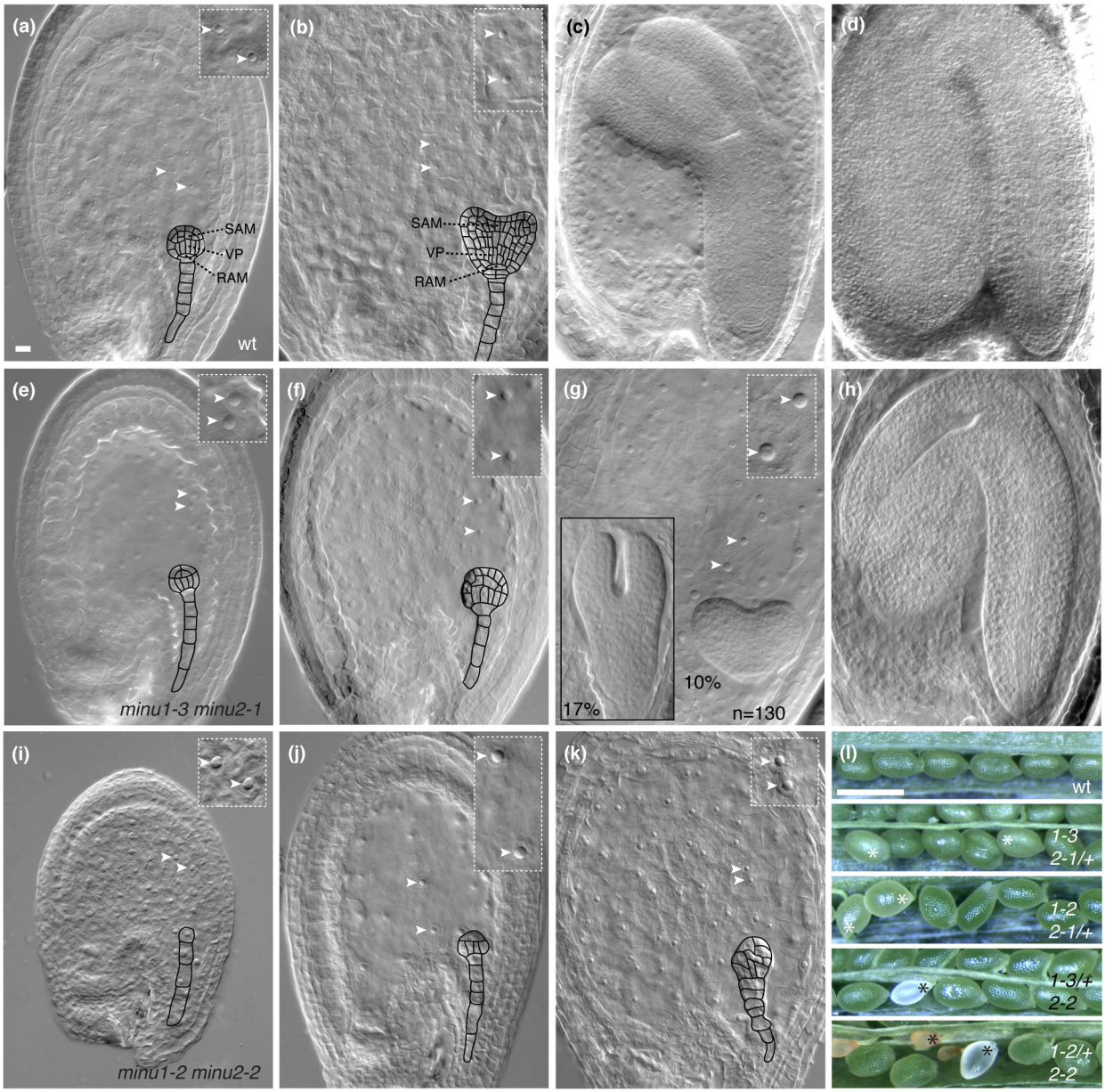

Figure 8. Embryo, endosperm, and ovule development in wild type and *minu1minu2* double mutants

(a–d) Wild-type embryos and endosperm at the globular (a), heart (b), late torpedo (c), and late bent cotyledon (d) stage of development. The SAM, vascular primordia (VP) and RAM are indicated with dotted lines. (e–h) *minu1-3 minu2-1* double mutant embryos and endosperm at the globular (e), heart (f), late torpedo (g), and late bent cotyledon (h) stage. The percentages of the two prevalent morphological phenotypes seen in the *minu1-3 minu2-1* allele combination are shown in the main panel and inset in (g). (i–k) *minu1-2 minu2-2* double mutant embryos and endosperm at the globular (i), heart (j) and late torpedo (k) stage. For the sake of clarity, cell outlines of early stage embryos are shown in black. Insets in panels (a), (b), (e), (f), (g), (i), (j), and (k) show endosperm nuclei (arrowheads) and

cell walls (in (a) and (b)) at 2x magnification. Siliques from wildtype and all four combinations of mutant alleles (l). Asterisks: shriveled or empty ovules due to embryo defects as shown in (k). Panels (a–k) are at equal magnification; scale bar (a) = 10 μm. Images in (l) are at equal magnification; scale bar = 0.5 mm.

Table 1

Quantification of defective embryo phenotypes segregating in all allelic combinations of single and double *minu1* and *minu2* mutants

genotype	globular	heart	torpedo	bent cotyledon
wild type	0.5% abn. (183)	0% abn. (92)	0.8% abn. (131)	0.4% early arrest (223)
minu1-2	1.4% abn. (281)	4.3% abn. (251)	0% abn. (122)	0.8% early arrest (233)
minu1-3	1.3% abn. (384)	1.7% abn. (178)	0.8% abn. (122)	0.4% early arrest (241)
minu2-1	1.5% abn. (335)	4.0% abn. (249)	2.6% abn. (190)	0.4% early arrest (244)
minu2-2	3.7% abn. (191)	1.4% abn. (205)	1.8% abn. (112)	0.4% early arrest (230)
minu1-2 minu2-1/+	26.2% abn. (160)	22.6% abn. (159)	25.5% abn. (243)	21.2% abn. SAM/RAM **1% globular arrest** (174)
minu1-3 minu2-1/+	18.7% abn. (331)	22.6% abn. (399)	25.8% abn. (502)	20.0% abn. SAM/RAM **0% globular arrest** (190)
minu1-2/+ minu2-2	**27% preglobular arrest** (285)	0.7% abn. **19.9% preglobular arrest** (301)	0.7% abn. **22.0% preglobular arrest** (150)	0.4% abn. **26.3% preglobular arrest** (254)
minu1-3/+ minu2-2	2% abn. **18.8% preglobular arrest** (191)	1.8% abn. **16% preglobular arrest** (162)	8.1% abn. **16.2% preglobular arrest** (259)	13.5% abn. SAM/RAM **12.4% preglobular arrest** (178)

abn.: abnormal (viable) embryo; n.d. not determined; brackets: n.